World Academy of Science, Engineering and Technology
International Journal of Electronics and Communication Engineering
Vol:10, No:10, 2016

Performance Evaluation of Distributed and Co-Located MIMO LTE Physical Layer Using Wireless Open-Access Research Platform

Ishak Suleiman, Ahmad Kamsani Samingan, Yeoh Chun Yeow, Abdul Aziz Bin Abdul Rahman

***Abstract*—**In this paper, we evaluate the benefits of distributed 4x4 MIMO LTE downlink systems compared to that of the co-located 4x4 MIMO LTE downlink system. The performance evaluation was carried out experimentally by using Wireless Open-Access Research Platform (WARP), where the comparison between the 4x4 MIMO LTE transmission downlink system in distributed and co-located techniques was examined. The measured Error Vector Magnitude (EVM) results showed that the distributed technique achieved better system performance compared to the co-located arrangement.

***Keywords*—**Multiple-input-multiple-output, MIMO, distributed MIMO, co-located MIMO, LTE.

I. Introduction

LONG Term Evolution (LTE) system is designed to serve the growth of mobile internet. It is usually referred to as the 4G system due to a significant performance improvement compared to the previous 3G system. The 3GPP has come out with this technological advancement in order to achieve higher data rate, while at the same time, improving the efficiency and coverage as well as reducing the operating cost [1] and [2].

One of the key reference signal that has been specified for enabling multiple-input multiple-output (MIMO) LTE downlink system is the Cell-specific Reference Signal (CRS). At the receiving User Equipment (UE), the CRS is used to estimate the propagation channels before data recovery, and decoding process can be performed. LTE downlink system uses the Orthogonal Frequency-Division Multiple Access (OFDMA) technique, where digital data are encoded on multiple carrier frequency with assigning subsets of subcarriers to individual users [3].

Performance comparison between the distributed MIMO systems and the co-located MIMO systems has been studied rigorously in literature. For example, in [4]-[8] the benefit of distributed MIMO system has been recognized in improving overall system capacity, compared to the co-located MIMO system. Nevertheless, the comparative works in [4]-[8] mainly focus on simulation and analytic works. In [4]-[6], the results are related to the Rayleigh channel, correlated fading and shadowing environments, and MIMO simulation for 5G system, respectively. In [7], [8], the results of simulation work on the ergodic rate performance for the downlink MIMO and cellular network were presented. In this contribution, we would like to highlight our experimental works using WARP, which verified the claim of performance superiority of the distributed MIMO system in the earlier publications. Particularly, a 4x4 MIMO LTE downlink physical (LTE DL PHY) layer system was considered in this investigation.

Ishak Suleiman, Ahmad Kamsani Samingan, Yeoh Chun Yeow, Abdul Aziz Bin Abdul Rahman are with the Signal Processing Lab., TM Research and Development Sdn. Bhd., Cyberjaya, Selangor, Malaysia (e-mail: ishak@tmrnd.com.my, drkamsani@tmrnd.com.my, yeow@tmrnd.com.my, abd_aziz@tmrnd.com.my).

With the assistance of the Wireless Open-Access Research Platform Lab (WARPLab) [9] framework for rapid physical layer prototyping, an LTE physical layer was implemented and studied. The WARP platform supports dual bands, namely 2.5 GHz and 5 GHz. Up to four radio transceivers are possible, each having 20 MHz signal bandwidth. Thus, an LTE downlink physical (DL PHY) modem can be implemented using this WARP platform in verification and testing the LTE DL PHY algorithm.

This paper is organized as follows. In Section II, we discuss about the 4x4 MIMO LTE DL PHY description. In Section III, the comparison between distributed and co-located 4x4 MIMO LTE DL PHY technique is explained. Section IV presents the WARP verification and test results and finally in Section V, concluding remarks are made together with suggestions for future works.

II. 4X4 MIMO LTE DL PHY Layer Description

As mentioned before, a single WARP board can implement up to four transceivers. Hence, in this work, three WARP boards are used to realize the distributed 4x4 MIMO technique, where two of those boards are used as MIMO transmitters, and the other board is used as the 4-antenna receiver. This arrangement is clearly shown in Fig. 1 (a). On the other hand, only two WARP boards are needed to implement the co-located 4x4 MIMO technique as depicted in Fig. 1 (b).

The 4x4 MIMO LTE DL PHY layer, which has been explained in [3] is made as our main reference. One subframe of 14 OFDM symbols is generated based on resource grid allocation as depicted in Fig. 2, where only the CRS and user data are mapped in the resource grid. Other types of channels such as the Primary Synchronization Channel (P-SCH), Secondary Synchronization Channel (S-SCH), Physical Broadcast Channel (PBCH), and Control Format Indicator (CFI) are excluded in this downlink implementation. The start of the radio frame is assumed to be perfectly known at receiver. Furthermore, the frequency offset introduced is being

pre-compensated at the transmitters. In real practical system, these issues are handled at the receiving terminal by using P-SCH signal. There are 96 Resource Elements (RE) reserved for CRS transmission in each Resource Block (RB) that implements four-antenna-port configuration. The remaining 576 REs of the resource grid are allocated for carrying user data per RB in a particular DL radio subframe. Thus, implementation of CRS imposes approximately 14.29% (96/672) overhead to the LTE system per RB.

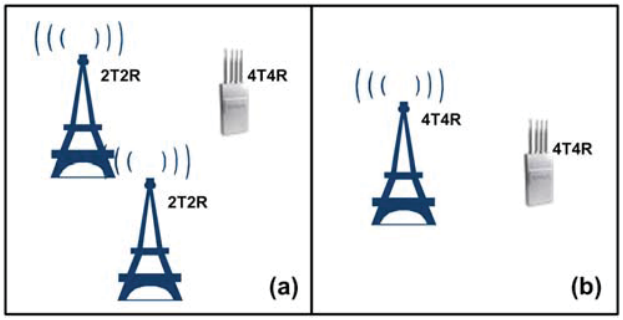

Fig. 1 (a) Distributed and (b) co-located 4x4 MIMO system in actual system realization

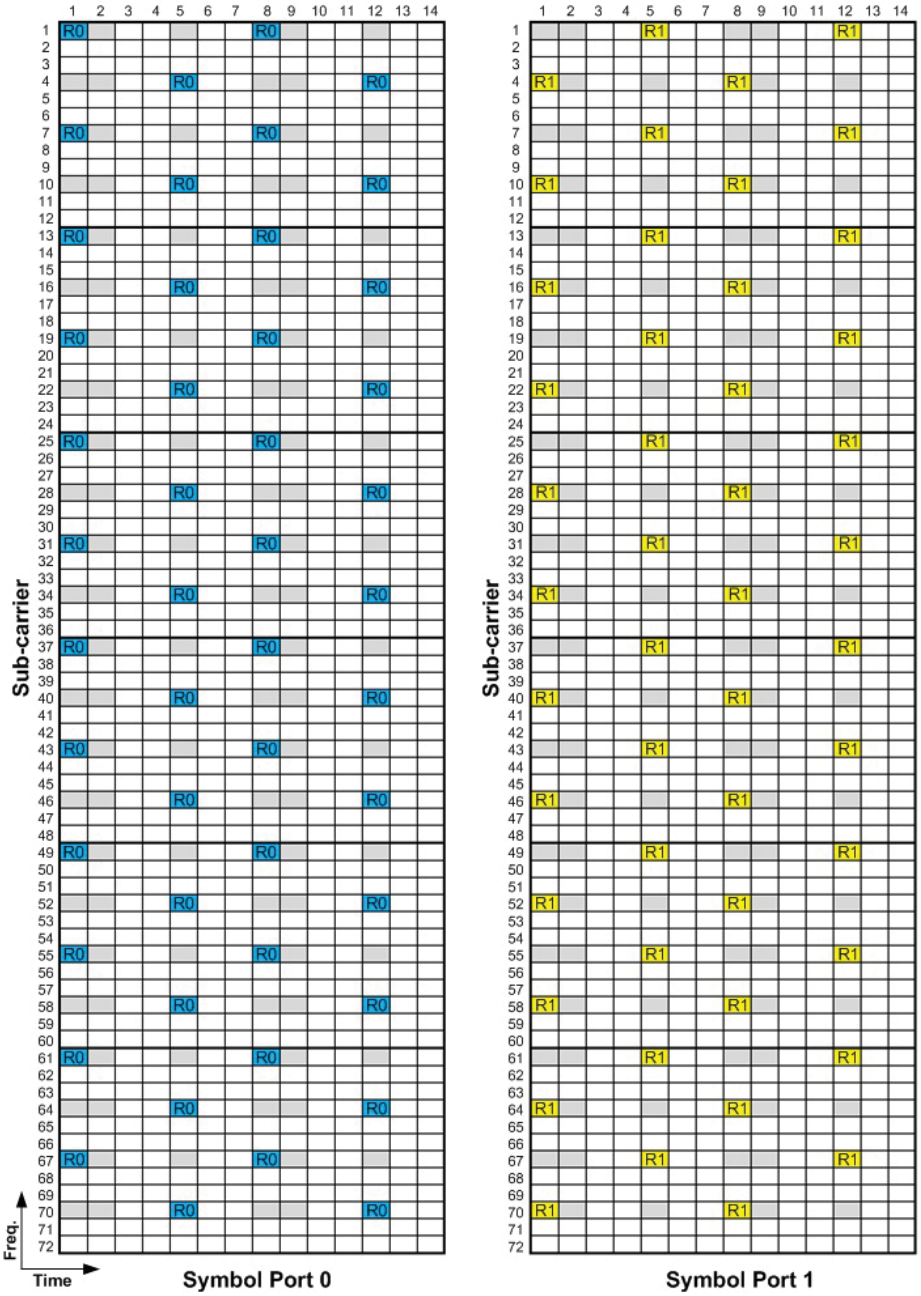

Fig. 2 (a) Downlink radio subframe structure (6-RB, 4 antenna port, without CFI) (Part 1)

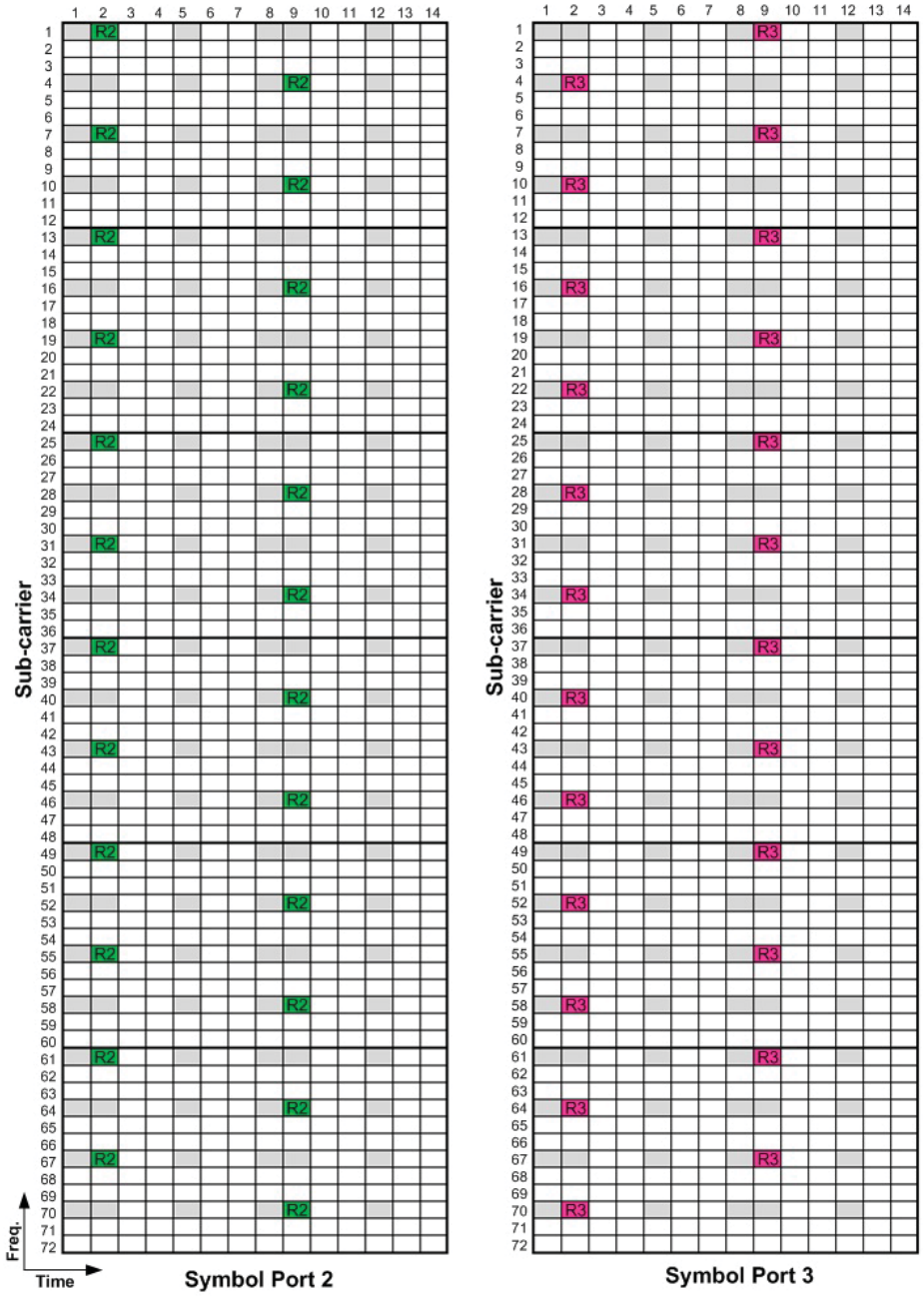

Fig. 2 (b) Downlink radio subframe structure (6-RB, 4 antenna port, without CFI) (Part 2)

The relationship between the signal bandwidth (*BW*), resource block (RB) and subcarrier spacing (Δf) is given in (1) [3]:

$$BW = 12\, N_{RB}\, \Delta f \quad (1)$$

where subcarrier spacing (Δf) is fixed at 15 kHz and the number of resource block (N_{RB}) is either 6, 15, 25, 50, 75, or 100.

The physical data rate calculation (bit/s) for our 4x4 MIMO LTE DL PHY system is given in (2),

$$data\_rate = 192\, \Delta f\, N_{RB}\, N_{mod}\, R / 5 \quad (2)$$

where Δf is 15k Hz, N_{RB} is the number of resource block (6, 15, 25, 50, 75 or 100-RBs), N_{mod} represents the number of QAM bit representation (2-bit for QPSK, 4-bit 16-QAM and 6-bit 64-QAM) and finally R is the coding-rate (1/2, 2/3 and 3/4).

Table I shows signal bandwidth (BW) and physical data rate based on (1) and (2) for a 64-QAM modulation scheme with 3/4 coding rate, with respect to resource block (RB) of 15 kHz subcarrier spacing (Δf).

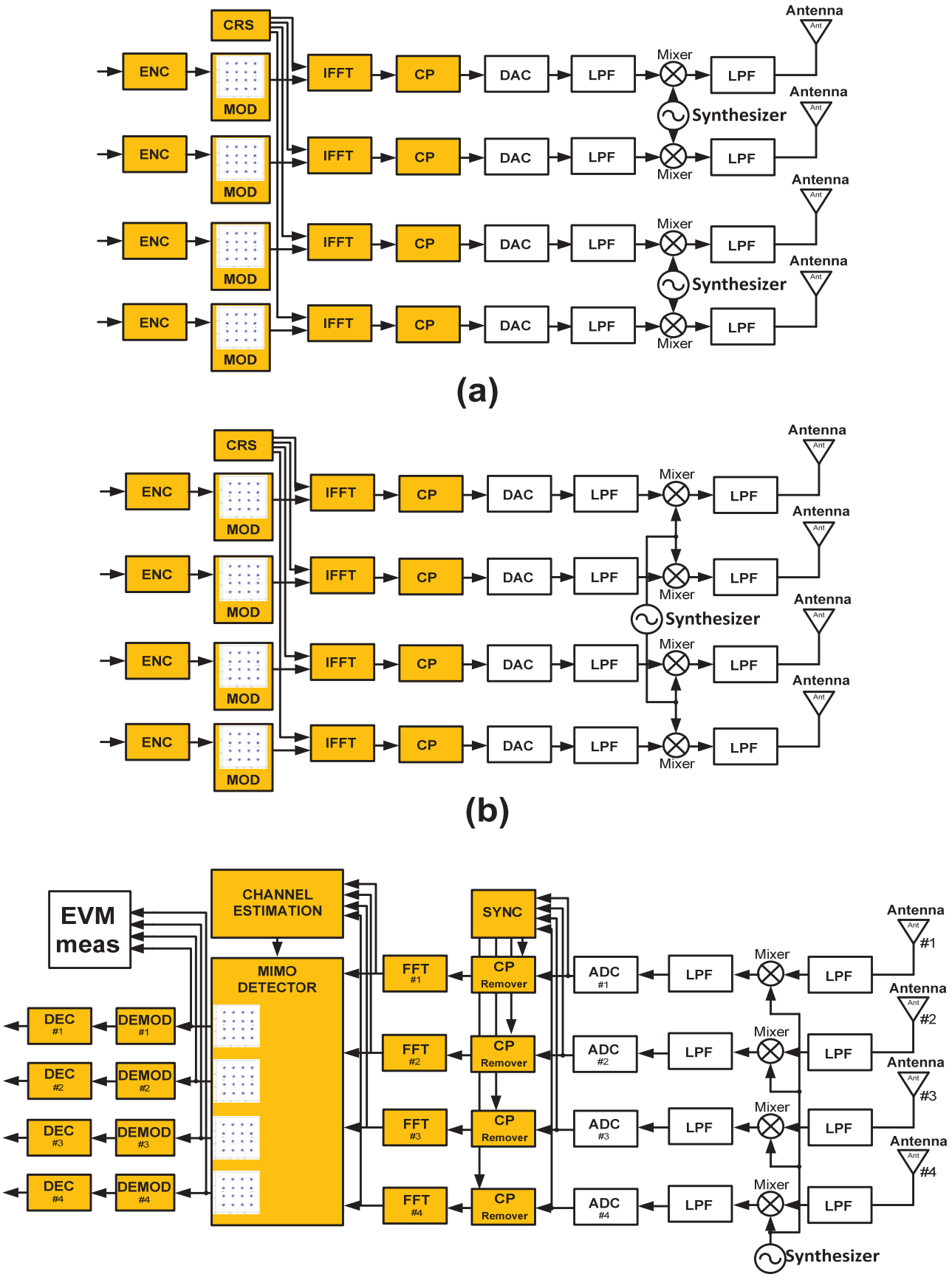

Fig. 3 The 4x4 MIMO LTE DL PHY layer architecture: (a) distributed and (b) co-located technique

TABLE I
SIGNAL BANDWIDTH (*BW*) AND PHYSICAL DATA RATE (N_{mod} = 64-QAM, R= 3/4, Δf=15kHz)

Number of Resource Block, (N_{RB})	Signal bandwidth, BW, (MHz)	*data_rate*, (Mbps)
6	1.1	15.6
15	2.7	38.9
25	4.5	64.8
50	9.0	129.6
75	13.5	194.4
100	18.0	259.2

Fig. 3 shows a block diagram of 4x4 MIMO LTE DL PHY layer architecture for (a) distributed, and (b) co-located 4x4 MIMO techniques. Both transmitters (a) and (b) use the same receiver structure for demodulating the 4x4 LTE DL PHY signals. The main difference between distributed and co-located technique, as shown in Fig. 3, is that the distributed technique requires two synthesizer modules or system clocks to operate. By contrast, the co-located technique requires only one synthesizer or system clock. The remaining block modules are the same for both scenarios.

III. COMPARISON BETWEEN DISTRIBUTED AND CO-LOCATED 4X4 MIMO LTE DL PHY TECHNIQUE

The architecture of the 4x4 MIMO LTE DL PHY technique as shown in Fig. 3 consists of Forward Error Correction (FEC) encoders (ENC), modulators (MOD), inverse fast Fourier transforms (IFFT), cyclic prefix (CP), Digital-to-Analog Converter (DAC), Low-pass filters, mixers, synthesizers, and antennas on the transmitter side. On the other side, the receiver consists of low-pass filters, synthesizers, mixers, ADC, CP remover, fast Fourier transform (FFT) modules, channel estimation module, MIMO detectors, demodulators and FEC decoders.

Encoder (ENC) block generates linear codewords such as convolutional encoder (CE), turbo encoder etc., so that error correction can be carried out at the receiving terminal. Detection errors within the codewords can either be fixed or at least significantly reduced at the receiver by using decoding algorithm such as Viterbi decoder, turbo decoder, and so on. On top of that, interleaving, data puncturing, and scrambler also been exploited in the encoder in order to improve the performance. Hence, coding rate (R) can be manipulated to have a desired data rate such as 1/2, 2/3, and 3/4, where the value indicates the ratio of the number of input bits to the number of output bits. For example, R=1/2 implies that for every one-bit data into the encoder, there will be two bits out of the encoder.

Modulator (MOD) is the bit to symbol mapping process for the modulation scheme such as QPSK, 16-QAM and 64-QAM. The choice of modulation scheme will determine the number of bits can be carried in one symbol, where two bits, four bits and six bits can be mapped to QPSK, 16-QAM and 64-QAM symbol, respectively. The higher the modulation order, the higher the system throughput (speed). However, this throughput improvement comes at the cost of lower noise resilience. The CRS signal will be transmitted by using the QPSK format and it is used for estimating the channel at the receiver. This CRS will be assigned into their respective resource element (RE) as shown in Fig. 2. Then, IFFT is invoked for transforming the frequency-domain symbols into the corresponding time-domain representation. After that, CP is inserted to the time-domain samples as protection from inter-symbol interference (ISI). Up to this stage, the process is carried out in digital domain.

Prior to transmission, the baseband digital signal is converted to the analogue domain by using Digital-to-Analogue Converter (DAC). The resultant analogue signal is filtered before mixed by using the synthesizer in order to generate the radio frequency (RF) signal. The RF signal is transmitted over the air trough antenna. The reverse process is done at the receiving terminal. The received baseband signal is equalized by using Zero-forcing technique to demodulate QAM symbols. Finally, Viterbi decoder/Turbo Decoder is used to recover back the transmitted message data.

We need to highlight here a practical issue pertaining the distributed 4x4 MIMO technique. Recall that two separate WARP boards, each implementing a two-port-antenna configuration, are combined together at the transmitter side. Hence, a four-antenna distributed transmitter is realized. Another point to note here is that each WARP board that functions as the transmitter is operating using different system clock and synthesizer, which in turn generates different frequency offset value at the receiver. Therefore, the challenge is how to mitigate these frequency offsets originating from two different sources at the user terminal. In fact, the demodulation process at receive terminal is very sensitive to the frequency offset.

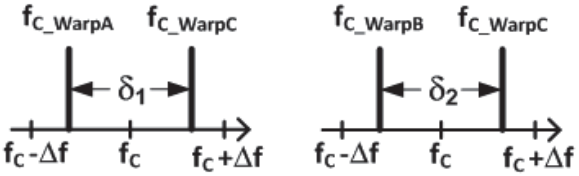

Fig. 4 Frequency offset illustration between WARP board A, B and C

In our experimental study, a procedure was proposed in order to overcome the frequency offset problem. An offline technique was used to estimate the frequency offset introduced by the two separate WARP boards as follows:

1. WARP transmitter board A will transmit training sequence and WARP receiver board C will estimate the frequency offset A. Let us denote this as δ_1.
2. WARP transmitter board B will transmit training sequence and WARP receiver board C will estimate the frequency offset B. Let us denote this value as δ_2.
3. Use the two estimated values δ_1 and δ_2 to pre-compensate the frequency offsets at the respective WARP transmitter boards, specifically after the CP insertion process.

The above procedure is also applied for the co-located 4x4 MIMO technique. However, only one frequency offset value needs to be estimated. Fig. 4 shows how frequency offset is

initiated in the real system caused by local oscillator (LO) frequency error for WARP board A, B, and C.

IV. WARP Verification and Test Result

In this section, detailed procedure on the experimental work involving the WARP boards will be explained. Firstly, the interested reader is recommended to refer the WARP documentation [9], particularly, the topic about hardware and software setup. The important hardware and software specifications are described in Table II.

TABLE II
WARP System Specifications

Items	Specification
Radio frequency	2.4/5 GHz, 4 port radio
ADC / DAC	12-bit, I/Q, 4 port
FPGA (Field Programmable Gates Array)	Virtex 6 (XC6VLX240T-2FFG1156C)
Buffer size	6.3 Mbits (32k samples x 12-bit x 2 (I/Q) x 4 (RFs) x 2 (Tx/Rx))
Ethernet Interface	2 gigabit Ethernet interface
WARPLab Reference Design	WARPLab_Reference_Design_7.4.0
MATLAB Software	Matlab R1012b
Number of WARP boards	3 units
Antenna	5dBi Indoor Omni-directional Antenna, 10 units
PC	Computer for centralized processing between WARP boards
Gigabit router	1 unit

Fig. 5 shows how WARP platform was setup for our experimental works. Specifically, Figs. 5 (a) and (b) show the setup for distributed and co-located 4x4 MIMO LTE DL PHY layer system, respectively. The experiment was conducted in an indoor lab environment, where the distance between transmitter and receiver is within radius 0.5 meters. The main radio parameters used are shown in Table III.

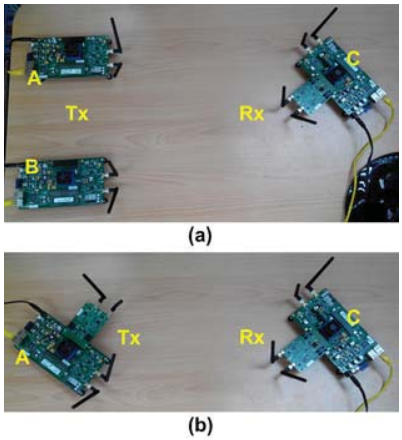

Fig. 5 WARP experimental setup for 4x4 MIMO LTE DL PHY layer system: (a) distributed and (b) co-located technique

A flowchart on how the experiment being conducted is depicted in Fig. 6. Firstly, the 4x4 MIMO LTE DL PHY baseband transmitter data was generated by using MATLAB software, assuming 64-QAM modulation and a total of 100 RBs. Then, if distributed scenario was selected, the four generated transmit data streams are buffered into WARP A RF1, WARP A RF2, WARP B RF1, and WARP B RF2, respectively. Otherwise for co-located experiment option, WARP A RF1, RF2, RF3, and RF4 are being selected. After that, a process was triggered to transmit and receive radio signal over the air concurrently, followed by retrieving the receive baseband signal from WARP C to the host PC. Finally, data recovery for the 4x4 MIMO LTE DL PHY baseband was carried out by using MATLAB.

TABLE III
WARP Radio Parameters

Items	Specification
Radio frequency	5.240 GHz
Tx baseband gain value	-5 dB
Tx RF gain value	15 dB
Rx baseband gain value	0.5 dB
Rx RF gain value	30 dB

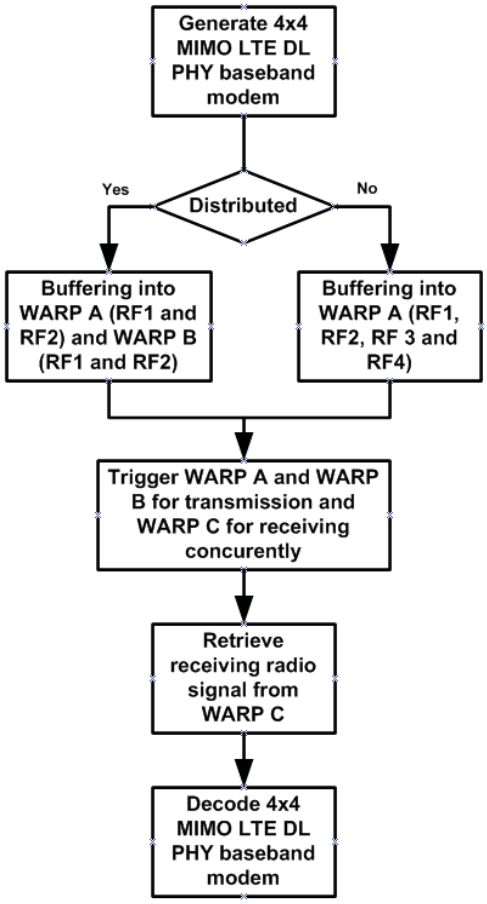

Fig. 6 Flowchart for distributed and co-located 4x4 LTE DL physical

The constellation result of the 4x4 MIMO LTE DL PHY layer system is shown in Fig. 7 for one subframe. Note that the modulation scheme is 64-QAM. The EVM distribution of 100 subframes data is shown in Fig. 8, and Table IV summarizes the results of the experiment.

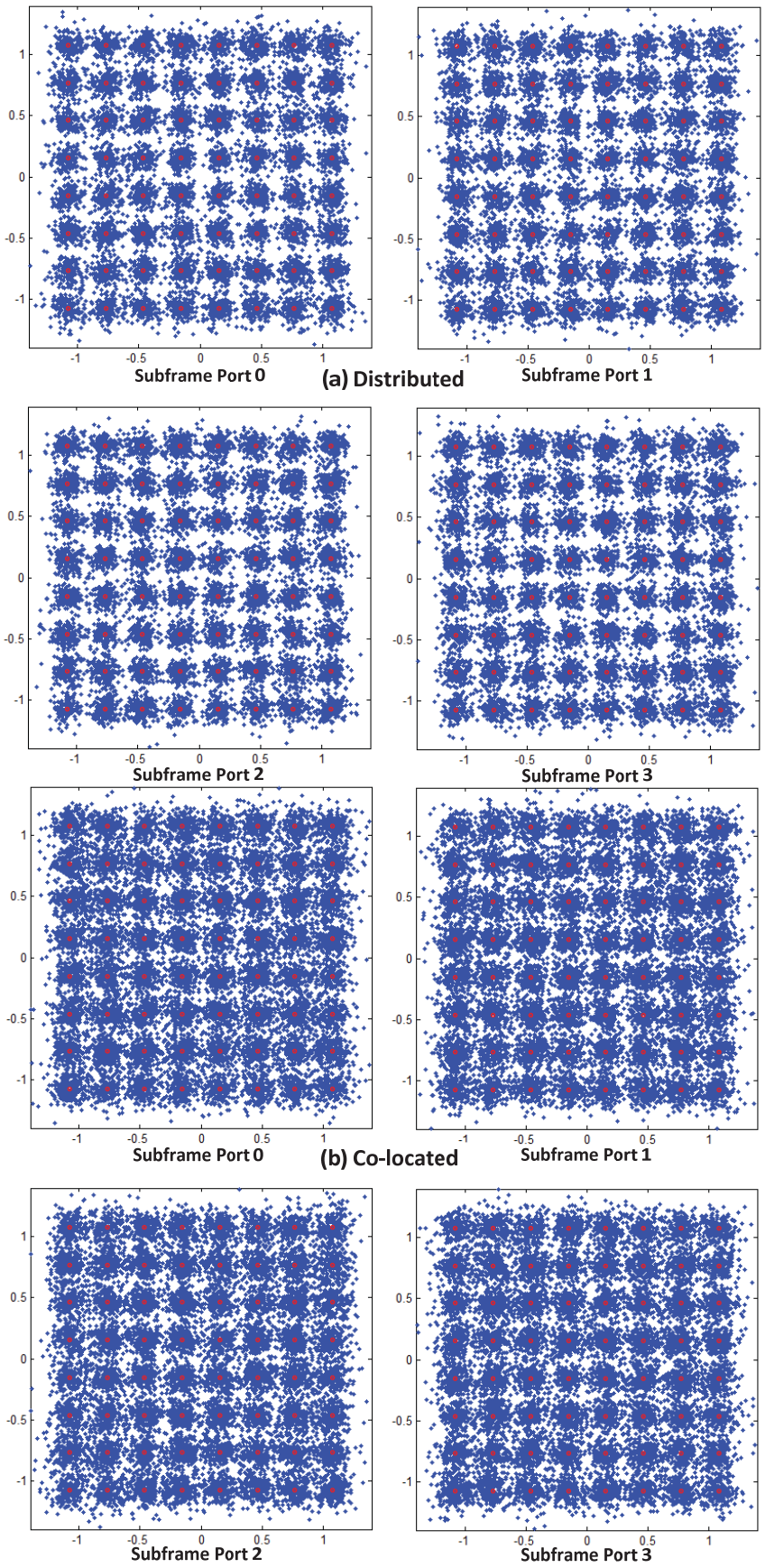

Fig. 7 Constellation of 64-QAM result of 4x4 MIMO LTE DL PHY layer system (a) distributed and (b) co-located

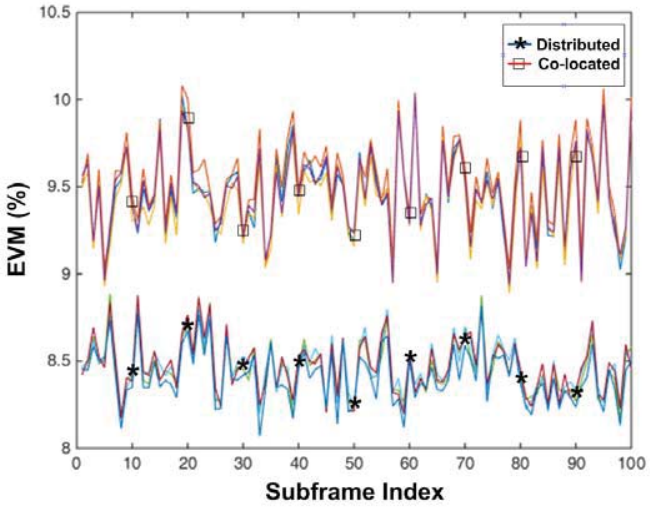

Fig. 8 Distributed and co-located EVM over 100 LTE subframes data

It is shown in Fig. 8 and Table IV that the distributed technique improves EVM around 1% compared to that of the co-located technique, thus improving the overall performance of the 4x4 MIMO LTE DL PHY layer system and closely meet specification requirements in [10].

TABLE IV
EVM SUMMARIZED RESULTS OF EACH PORT BASED ON 100 LTE SUBFRAMES

	Port 0	Port 1	Port 2	Port 3
Distributed:-				
Mean EVM (%)	8.4610	8.4733	8.4740	8.4127
Co-located:-				
Mean EVM (%)	9.4615	9.5236	9.4304	9.4649

V. CONCLUSION

System performance improvement can be achieved by increasing the physical separation between the antennas. This has been proven in the experimental setup by using WARP board, where the distributed 4x4 MIMO LTE system, having greater antenna separation, exhibited better performance compared to the co-located technique. Our future works will investigate various real-time frequency offset estimation algorithms and compensation techniques that can potentially be integrated into our platform in order to make it a step closer to the practical scenario.

ACKNOWLEDGMENT

This work is supported by Telekom Malaysia (TM) research grant of Inter-Cell MIMO Long Term Evolution (RDTC/150877) project.

REFERENCES

[1] S. Abeta, "Toward LTE commercial launch and future plan for LTE enhancements (LTE-Advanced)," in Communication Systems (ICCS), 2010 IEEE International Conference, pp. 146 - 150, 2013.
[2] A. Gosh, and R. Ratasuk, "Essentials of LTE and LTE-A (The Cambridge Wireless Essentials Series)," Cambridge University Press, Cambridge, 2011.
[3] 3GPP TS 36.211, V11.0.0, "3rd Generation Partnership Project; Technical Specification Group Radio Access Network; Evolved Universal Terrestrial Radio Access (E-UTRA); Physical Channels and Modulation (Release 11)," September 2012.
[4] C. He, B. Sheng, P. Zhu and X. You, "Energy Efficient Comparison between Distributed MIMO and Co-located MIMO in the Uplink Cellular Systems," in Vehicular Technology Conference (VTC Fall), 2012 IEEE Conference, pp. 1-5, 2012.
[5] H. Dai, "Distributed Versus Co-Located Mimo Systems with Correlated Fading and Shadowing," in Acoustics, Speech and Signal Processing, ICASSP 2006 Proceedings, 2006 IEEE International Conference, pp. IV - IV, 2006.
[6] D. Qiao, Y. Wu and Y. Chen, "Massive MIMO architecture for 5G networks: Co-located, or distributed?," in Wireless Communications Systems (ISWCS), 2014 11th International Symposium, pp. 192-197, 2014.
[7] Z. Liu and L. Dai, "Asymptotic capacity analysis of downlink MIMO systems with co-located and distributed antennas," in Personal Indoor and Mobile Radio Communications (PIMRC), 2013 IEEE 24th International Symposium, pp. 1286-1290, 2013.
[8] Z. Liu and L. Dai, "A Comparative Study of Downlink MIMO Cellular Networks with Co-Located and Distributed Base-Station Antennas," in IEEE Transactions on Wireless Communications, pp. 6259 - 6274, 2014.
[9] WARP v3 User Guide https://warpproject.org/trac/wiki/WARPLab/Downloads.
[10] 3GPP TS 36.104 V11.2, "Technical Specification Group Radio Access Network; Base Station (BS) radio transmission and reception, (Release 11.2), " November 2012.